Ab initio simulations of pseudomorphic silicene and germanene bidimensional heterostructures

Alberto Debernardi[1,*] and Luigi Marchetti[1,2]
[1]*CNR-IMM, sede Agrate Brianza, via Olivetti 2, I-20864, Agrate Brianza, Italy*
[2]*Universitá degli studi di Milano, via Celoria 16, I-20133, Milano, Italy*
(Received 4 January 2016; revised manuscript received 28 May 2016; published 21 June 2016)

Among the novel two-dimensional (2D) materials, silicene and germanene, which are two honeycomb crystal structures composed of a monolayer of Si and Ge, respectively, have attracted the attention of material scientists because they combine the advantages of the new 2D ultimate-scaled electronics with their compatibility with industrial processes presently based on Si and Ge. We envisage pseudomorphic lateral heterostructures based on ribbons of silicene and germanene, which are the 2D analogs of conventional 3D Si/Ge superlattices and quantum wells. In spite of the considerable lattice mismatch (∼4%) between free-standing silicene and germanene, our *ab initio* simulations predict that, considering striped 2D lateral heterostructures made by alternating silicene and germanene ribbons of constant width, the silicene/germanene junction remains pseudomorphic—i.e., it maintains lattice-matched edges—up to critical ribbon widths that can reach some tens of nanometers. Such critical widths are one order of magnitude larger than the critical thickness measured in 3D pseudomorphic Si/Ge heterostructures and the resolution of state-of-the-art lithography, thus enabling the possibility of lithography patterned silicene/germanene junctions. We computed how the strain produced by the pseudomorphic growth modifies the crystal structure and electronic bands of the ribbons, providing a mechanism for band-structure engineering. Our results pave the way for lithography patterned lateral heterostructures that can serve as the building blocks of novel 2D electronics.

DOI: 10.1103/PhysRevB.93.245426

I. INTRODUCTION

Silicene and germanene, which are graphenelike structures composed of Si and Ge, respectively, are attracting increasing interest in the material science community due to their potential applications in the new generation of electronic devices based on bidimensional sheets consisting of one (or few) monolayer(s) (MLs). The high surface/volume ratio of these two-dimensional (2D) compounds make them ideal candidates for sensor applications, H-storage [1], or ultrascaled electronics, which can benefit from novel physical phenomena arising in two dimensions, such as quantum confinement effects or topological protected electronic states [2].

With respect to other 2D materials, such as MoS_2 or graphene, silicene and germanene can benefit from the compatibility with industrial processes presently based on Si and Ge technology. Like graphene, silicene and germanene have honeycomb crystal structures made up of 1 ML of Si and Ge, respectively. Unlike graphene, silicene and germanene have a buckled planar structure due to a mixed sp^2-sp^3 hybridization.

Although silicene and germanene do not exist in nature in free-standing form, they can be engineered on appropriate substrates that stabilize a 2D honeycomb crystal structure. Recent reviews about the state of the art of silicene and germanene technology and the potential application of these 2D compounds for ultimate thickness scaling in electronics can be found in Refs. [3–5]. A germanene layer was recently synthesized on Al(111) [6], while several experiments proved the formation of silicene nanoribbons (NRs) and sheets on silver surfaces [3–5]. Because interaction with a metallic substrate modifies the structural and electronic properties of silicene, a considerable amount of effort is presently underway to synthesize and characterize silicene and germanene on semiconducting or insulating substrates, in order to obtain silicene or germanene sheets whose electronic states are not hybridized with the surface states of the substrate [3]. The integration of these 2D materials in nanoelectronics is presently underway: a silicene field-effect transistor operating at room temperature was recently reported [7].

Free-standing silicene and germanene are predicted to be stable in a buckled monolayer, due to a mixed sp^2-sp^3 hybridization [8,9]. Like graphene, free-standing silicene and germanene are semimetals, and their electronic band structures present a Dirac cone at the K point of the Brillouin zone (BZ), with the Fermi energy located at the tip of the Dirac cone. As a consequence, charge carriers—electrons at the bottom of the upper cone or holes at the top of the lower cone, which can be generated by thermal excitation, impurity doping [10], an electric field [11], or other means—resemble massless Dirac fermions. The Dirac cone is responsible for the high mobility of carriers in graphene, with a Fermi velocity, v_F, of the order of 10^6 m/s [4]; similar Fermi velocities are expected for free-standing silicene and germanene [4].

Although Si and Ge share with C the same column of the Periodic Table, and they have electronic properties similar to C, they also exhibit peculiar features that may make them useable in the new 2D electronics: since Si and Ge are miscible, it is possible to form a crystalline random alloy [12] $Si_{1-x}Ge_x$, in which the Ge concentration x can vary from 0 to 1; by epitaxial growth on $Si_{1-x}Ge_x$ substrates, it is possible to build Si/Ge quantum wells or short-period Si/Ge superlattices by alternating pseudomorphic Si and Ge layers that match their lattice parameters parallel to the Si/Ge interface. By varying the

*alberto.debernardi@mdm.imm.cnr.it

superlattice period and the lattice parameters of the substrate, one can tailor and tune the electronic properties of the epitaxial layers.

We exploit this scenario in two dimensions, envisaging 2D pseudomorphic heterostructures (2D-PHs) formed by joining in-plane silicene and germanene ribbons; these 2D-PHs are the analogs of the usual 3D-Si/Ge superlattices and quantum wells, which have been studied extensively in recent decades [12].

In our case, instead of a 3D "substrate" we have a 2D "seed ribbon" (or, in analogy to the term used in three dimensions, a 2D substrate) that in our simulation is ideally replaced by an infinitely extended semiplane, which approximates a ribbon or a flake of macroscopic area. Instead of a 3D "interface" we have a 2D "interedge" (or a 2D interface) marking the junction between silicene and germanene. Instead of a 3D "epitaxial layer" we have a 2D "epitaxial ribbon" (in short an epi-ribbon), whose lattice parameter parallel to the interedge (2D interface) matches the lattice parameter of the seed ribbon (2D substrate) due to the pseudomorphic growth condition.

For the convenience of the reader who is unfamiliar with the new terminology introduced to describe 2D pseudomorphic growth, we choose to display in parentheses after the new term the equivalent term that is commonly used for 3D systems with the prefix 2D, so the term "interedge" will be followed by "(2D interface)," and the term "seed-ribbon" will be followed by "(2D substrate)."

In Figs. 1 and 2 we display the top (bottom panels) and the side (top panels) view of two of the heterostructures studied in the present work: in Fig. 1 we display the zigzag interedge (2D interface) between germanene (red atoms) epi-ribbon growth on a silicene (blue atoms) seed ribbon (2D substrate); in Fig. 2 we display the armchair interedge (2D interface) between silicene epi-ribbon growth on a germanene seed ribbon (2D substrate). Note that the lattice parameter of the seed ribbon (2D substrate) corresponds to its free-standing value, while the lattice parameter of the epi-ribbon is strained, as will be discussed in detail in Sec. III.

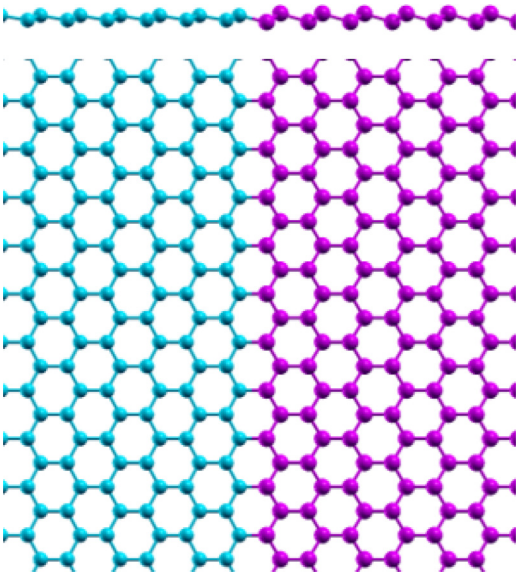

FIG. 1. Side view (top panel) and top view (bottom panel) of the 2D crystal structures used to simulate zigzag interedges (2D interfaces).

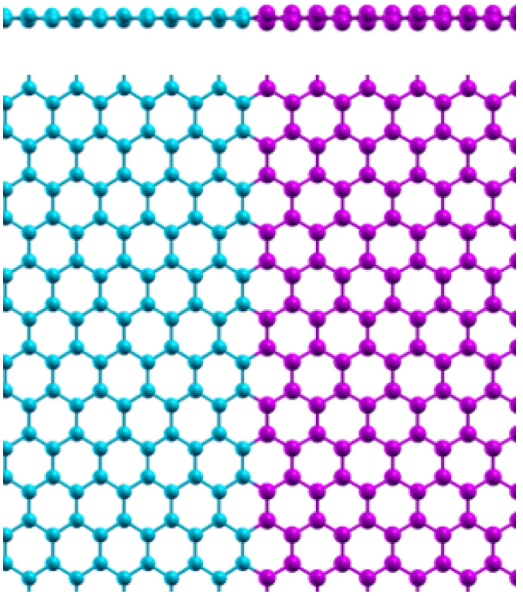

FIG. 2. Side view (top panel) and top view (bottom panel) of the 2D crystal structures used to simulate armchair interedges (2D interfaces).

The experimental realization of these 2D heterostructures is a difficult task, due to the lack of an in-plane growth technique that, starting from flakes or ribbons of silicene (or of germanene), is capable of growing germanene (silicene) ribbons *ex margine* [13], i.e., from the edge of a silicene (germanene) flake, controlling their size, shape, and width by an edge-by-edge deposition that is the 2D analog of chemical vapor deposition (CVD) or molecular beam epitaxy (MBE), techniques that are commonly used to produce 3D superlattices and quantum wells.

However, the planar geometry of the heterostructure allows us, at least in principle, to employ lithographic techniques to carve these new heterostructures out of 2D ribbons. To illustrate this possibility, in the following we briefly sketch step-by-step a possible growing sequence. As deposited, a germanene (or a silicene) flake, which has to be used as seed ribbon, is expected to present a shape having irregular edges, or, in some specific cases, to present a shape that is determined by the thermodynamics of growth processes, and which may be different from the shape needed for electronic applications. The first step is shaping the seed ribbon. To produce 2D-PHs, we suggest that lithography can be used to carve from the original flake a seed ribbon having edges with the desired orientation (zigzag or armchair, according to the case studied in the present work) and the desired width. The second step is *ex margine* growth of the epi-ribbon. From the edges of the existing germanene (silicene) flakes, we imagine growing a silicene (germanene) epi-ribbon, which is pseudomorphic to the germanene (silicene) seed ribbon, and it maintains regular edges at the interedge (2D interface) between silicene and germanene with the desired orientation (zigzag or armchair), as carved by lithography. At the end of the growth process, the pseudomorphic silicene (germanene) epi-ribbon has a sharp

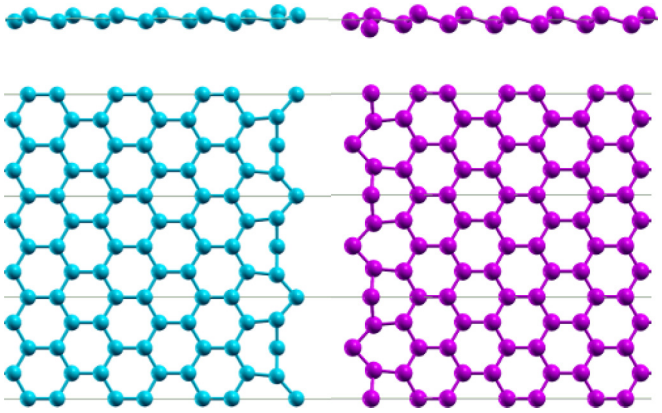

FIG. 3. Side view (top panels) and top view (bottom panels) of the 2D crystal structures used to simulate the zigzag surface edges.

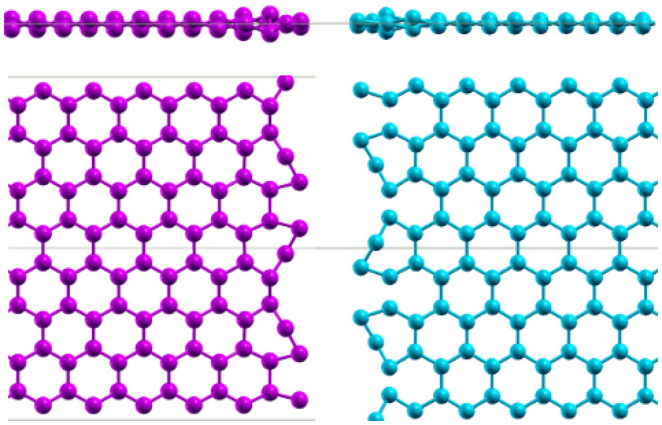

FIG. 4. Side view (top panels) and top view (bottom panels) of the 2D crystal structures used to simulate the armchair surface edges.

interedge (2D interface) with germanene (silicene), while the edge of the epi-ribbon not in contact with germanene can have an arbitrary shape and/or orientation. The third step is shaping the epi-ribbon. The edge of the silicene (germanene) epi-ribbon not in contact with germanene (silicene) is carved by lithography to obtain the desired orientation of the edge, and to produce a silicene (germanene) epi-ribbon having the desired width. The repetition of the second and third steps, i.e., alternating between an epi-ribbon of silicene and an epi-ribbon of germanene, produces a 2D-PH that is the 2D analog of a 3D Si/Ge superlattice (while stopping at the third step may produce a 2D analog of a 3D quantum well) [14]. Thus, the possibility of successfully growing 2D heterostructures is closely linked to the precision and resolution of present and near-future lithography.

In this framework, a crucial point is the determination of the maximum width that a germanene (silicene) ribbon can reach when it is pseudomorphically grown *ex margine* from a seed ribbon (2D substrate) of silicene (germanene), maintaining a lattice-matched interedge (2D interface) at the silicene/germanene junction. In fact, when the width of the epi-ribbon reaches a critical value w_c, it is energetically convenient for the 2D-PHs to break off the interedge (2D interface) bonds, thus forming two separate surface edges, and to release the strain energy of the epi-ribbon. In Figs. 3 and 4 we display the reconstructed surfaces for the zigzag and armchair edge, respectively. The lattice parameter parallel to the edge corresponds to a free-standing structure, and therefore the figure simulates a ribbon of silicene or of germanene of macroscopic size, when it has reached its critical width after pseudomorphic growth on zigzag- or armchair-oriented seed ribbons (such as those shown in Figs. 1 and 2). An illustrative scheme of this 2D pseudomorphic growth is displayed in the first (germanene epi-ribbon from silicene seed ribbon) and fourth (silicene epi-ribbon from germanene seed ribbon) column in Fig. 5.

In the present work, we used plane-wave pseudopotential techniques to compute the structural and electronic properties of silicene/germanene 2D-PHs. Remarkably, we show that a germanene (silicene) epi-ribbon can be grown *ex margine* from a silicene (germanene) seed ribbon (2D substrate) with a width several times larger than the resolution of state-of-the-art lithographic techniques, paving the way for new-conception heterostructures, lithographically patterned, for high-density 2D electronics.

II. COMPUTATIONAL METHODS

We simulated silicene and germanene heterostructures using the plane-wave pseudopotentials techniques, as implemented in the QUANTUM ESPRESSO (5.0.2) package [15]. In our calculations, we used the supercell method with periodic (Born–von Karman) boundary conditions. The distance between one atomic plane and its (periodically repeated) image is about 2 nm or greater, to ensure a decoupling between the wave function of different planes. Our supercells have 64 atoms to simulate the silicene/germanene interfaces and 68 atoms

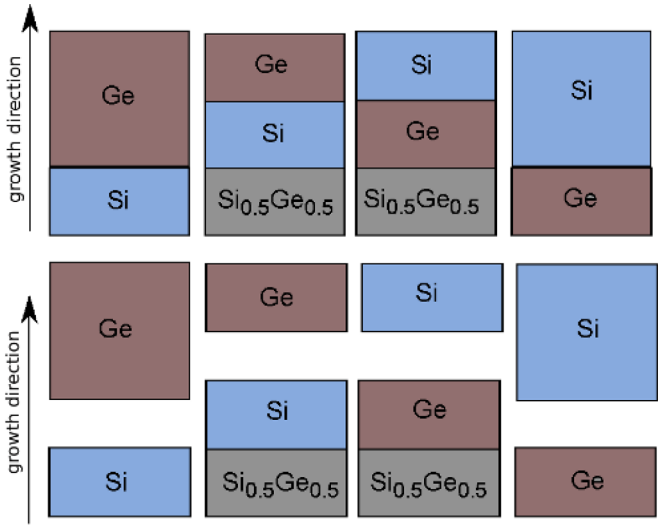

FIG. 5. Illustrative scheme of the critical width of the epi-ribbon. Top panel: seed ribbons, sketched as rectangles at the base of each of the fourth columns, have their free-standing lattice parameter. The epi-ribbons, sketched as rectangles on the top of the seed ribbons, have strained lattice parameters. Bottom panel: the same system as in the bottom panel when the epi-ribbons reach the critical width; the breaking of bonds at the interedge produces the relaxation of epi-ribbons to their free-standing lattice parameter.

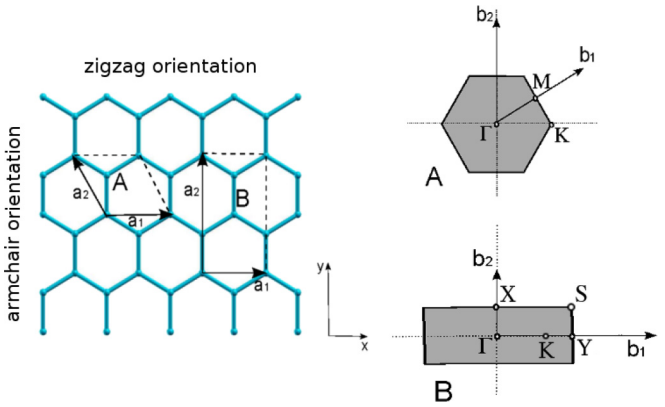

FIG. 6. Top view of the honeycomb crystal structure of silicene or of germanene (left panel) with the hexagonal (A) and rectangular (B) unit cells used to simulate the free-standing and strained crystal, respectively. The corresponding two-dimensional first Brillouin zones are displayed in the right panels.

to simulate the silicene or the germanene surfaces. Typical supercell structures used in the simulation are displayed in Figs. 1, 2, 3, and 4. For the simulation of zigzag and armchair interedges we use a rectangular supercell, whose side parallel to the interedge corresponds to the side of the rectangular unit cell of the bulk lattice displayed in Fig. 6 (B), while the side of the supercell perpendicular to the interedge is built by joining a ribbon of silicene and a ribbon of germanene, where each ribbon is obtained by repeating eight times the bulk unit cell along the growth direction [see Fig. 6 (B)]. The distance between two edges of the ribbon is $\sim$3 nm or greater.

To simulate the surface edge of both zigzag and armchair edges, we used supercells whose side parallel to the surface edge is twice the side of the rectangular bulk cell of Fig. 6 (B) to take into account the (2×1) surface-edge reconstruction [8]. For the side of the supercell perpendicular to the edge, we used a silicene (germanene) slab composed of a silicene (germanene) ribbon obtained by repeating eight times the bulk unit cell along the growth direction (i.e., the direction perpendicular to the surface edge); between a ribbon and its periodically repeated images (due to the use of Born–von Karman periodic boundary conditions) we put a slab of vacuum of at least 2 nm to ensure complete decoupling between the ribbon edges.

Our data for relaxed free-standing surfaces reproduce those of Ref. [8]. The edge and interedge (2D interface) energies are computed by varying the seed ribbon (2D substrate) lattice parameters [at least five different values are considered in the range of $a_{\parallel}(x)$] and fitted with a polynomial to extract the dependence on x in the whole range.

For all systems, the atomic positions are fully relaxed. The ground state was computed with the generalized gradient approximation [16] (GGA) to density functional theory scheme [17,18] with ultrasoft pseudopotentials [19,20]. We used a 35 Ry cutoff for the wave functions, and a 400 Ry cutoff for the augmentation density. Reciprocal space integration was performed using special point techniques with a (12,6,1) Monkhorst-Pack [21] grid for the rectangular Brillouin zone (four atoms per unit cell) of Fig. 6, while the grid was modified accordingly for the supercell to maintain an (approximately) equally spaced mesh. We estimated the error on the total energy to be lower than 0.1 mRy (i.e., $\sim$1 meV) per atom. Since silicene and germanene are semimetals, we used a small Gaussian broadening of 1 mRy (i.e., of $\sim$13.6 meV) to improve convergence. Convergence tests and further computational details can be found in Ref. [22].

III. STRAINED BULK

An epi-ribbon pseudomorphically grown from a seed ribbon (2D substrate) having a different lattice parameter is strained. Strain has been proposed as a suitable way to tune silicene and germanene band structures (also in combination with an electric field) [23], to modify the thermal conductivity of silicene [24,25], and to engineer the Fermi velocities of carriers within the Dirac cone [26]. For the latter property, a crucial point is to determine, in the range of strain considered, how the electronic band structure is modified, and if a transition from semimetal to metal can occur, thus degrading the high velocity carriers at the Fermi level, which are present within the Dirac cone in the semimetal state. While several works have considered biaxial strain as a means to tune the electronic structure [23,27–29], only a few have considered the effect produced by an uniaxial strain [26,30] on the band structure, which is the kind of strain we have to evaluate in the study of pseudomorphic 2D-PHs. In the following, we study the effects of pseudomorphic growth on the structural and electronic properties of wide ribbons in the region far from the ribbon edges. In this region, the epi-ribbon is conveniently described by a strained bulk unit cell. The lattice parameter of the epi-ribbon that is parallel to the interedge (2D interface), $a_{\parallel}$, is kept fixed to match the lattice parameter of the seed ribbon (2D substrate) and thus to mimic the pseudomorphic growth conditions, while the lattice parameter of the epi-ribbon perpendicular to the interedge (2D interface), $a_{\perp}$, is free to relax. According to our simulation (theoretical data taken from the literature [3] are in parentheses for comparison), the lattice parameters of free-standing silicene and germanene are $a_{\text{2D-Si}} = 3.87$ Å (3.83 Å) and $a_{\text{2D-Ge}} = 4.05$ Å (3.97 Å), respectively, while the buckling of free-standing silicene is $b_{\text{2D-Si}} = 0.44$ Å (0.44 Å) and the buckling of free-standing germanene is $b_{\text{2D-Ge}} = 0.69$ Å (0.65 Å).

In a silicene (or a germanene) epi-ribbon, the strain lifts the hexagonal symmetry of the free-standing primitive unit cell (see cell A in the left panel of Fig. 6). We consider the pseudomorphic growth of silicene (germanene) epi-ribbons on seed ribbons (2D substrate) with zigzag or armchair edges. With this constraint, the resulting unit cell of strained bulk silicene (germanene) has four atoms in the unit cell and rectangular symmetry (see cell B in the left panel of Fig. 6).

To tailor the band structure of 2D-PHs composed of silicene and germanene ribbons of different width, we considered the effect produced by the variation of the lattice parameters of the seed ribbon (2D substrate). To achieve, in an experiment, the tuning of $a_{\parallel}$, we suggest three different ways: (a) by stress, considering a germanene epi-ribbon laterally grown from a silicene seed ribbon (2D substrate) and applying a (mechanical) tensile uniaxial stress parallel to interedge (2D interface); (b) by geometry, alternating pseudomorphic stripes

of silicene and germanene having appropriate and constant width (in this case, $a_{\parallel}$ depends on the relative width of the two stripes; this planar heterostructure is the 2D analog of conventional 3D Si/Ge superlattices); and (c) by a 2D SiGe random alloy, envisaging a seed ribbon (2D substrate) composed of a $Si_{1-x}Ge_x$ alloy having a 2D honeycomb structure in which the Ge replaces randomly the Si sites of the silicene structure. By varying the Ge concentration, x, in 2D-$Si_{1-x}Ge_x$ we can tune the lattice parameter of the seed ribbon (2D substrate). The variation of the seed ribbon (2D substrate) lattice parameter is assumed to follow Vegard's law, according to the equation [31]

$$a_{\parallel}(x) = a_{\text{2D-Si}} * (1 - x) + a_{\text{2D-Ge}} * x. \quad (1)$$

In case (c), two ribbons, one of germanene and the other of silicene, are grown in sequence *ex margine* from a 2D-$Si_{1-x}Ge_x$ seed ribbon (2D substrate), each ribbon having the $a_{\parallel}$ equal to the lattice parameter of the 2D-$Si_{1-x}Ge_x$ alloy. This scheme is illustrated in the central panels of Fig. 5.

In 2D-$Si_{1-x}Ge_x$, $a_{\parallel}$ ranges from the lattice parameter of free-standing silicene to that of free-standing germanene. Since the properties of silicene (germanene) strained bulk are determined only by the parameter $a_{\parallel}$, we find it convenient, in the following, to use x to denote the value of the lattice parameter parallel to the interface $a_{\parallel}(x)$, as defined in Eq. (1); for $x = 0$ we deal with a 2D-PHs pseudomorphic growth on a silicene seed ribbon (2D substrate); for $x = 1$ we deal with a 2D-PHs pseudomorphic growth on a germanene seed ribbon (2D substrate). The results for $0 \leqslant x \leqslant 1$ are valid irrespective of the physical mechanism (a, b, or c) used to tune $a_{\parallel}$.

A planar compressive stress applied to a 2D layer is expected to produce a corrugation or a bowing of the whole sheet; on the contrary, a planar tensile stress applied to a 2D layer deforms the sheet, keeping the planar geometry. This makes it worthwhile to consider silicene/germanene pseudomorphic heterostructures under tensile strain, at values of $a_{\parallel}$ larger than that of germanene (i.e., for $x > 1$). Further, as it will be shown below, since the band structure of strained silicene presents the Dirac cone also for $a_{\parallel}$ equal to the lattice parameter of germanene, we have considered a slightly larger range for the seed ribbon (2D substrate) lattice parameter, namely $x \in [0,5/4]$.

To illustrate the effect of pseudomorphic growth on the band structure in the range of strain in which we are interested, in Fig. 7 we display the electronic band structure of strained bulk silicene (germanene), laterally growth on a seed ribbon (2D substrate) of germanene (silicene) having zigzag (top panels) or armchair (bottom panels) interedges (2D interface). The band structures of free-standing silicene and germanene are displayed for reference (as dashed lines).

As it can be immediately noticed from Fig. 7, the band structures of both silicene and germanene present a Dirac cone at the K point in the whole range of strain considered, while the slope of the Dirac cone (i.e., the Fermi velocity) is slightly modified by the strain. In the band structures of free-standing silicene and germanene, the Fermi energy is chosen as the zero of the energy scale in the figure, and it corresponds to the

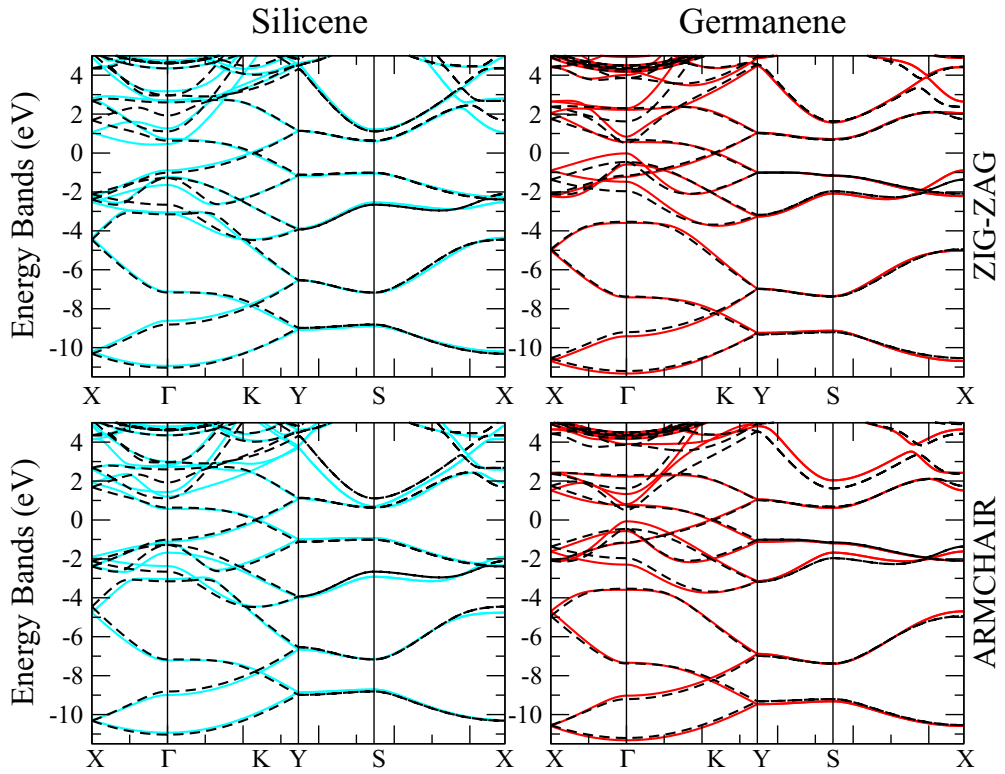

FIG. 7. The band structure of strained bulk silicene at $x = 1$ (left panels) and germanene at $x = 0$ (right panels) for zigzag (top panels) and for armchair (bottom panels) interedges (2D interfaces). $x = 0$ and 1 correspond to lateral growth from a silicene or a germanene free-standing seed ribbon, respectively. Black dashed lines correspond to the free-standing structure.

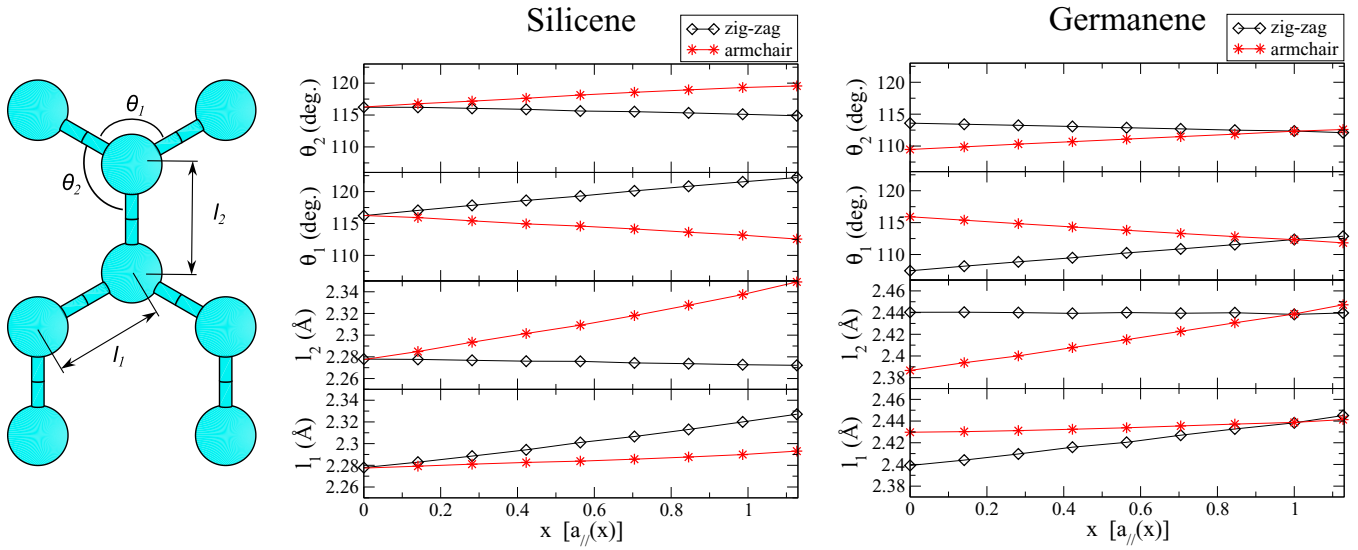

FIG. 8. Buckling parameters of strained bulk silicene and germanene as a function of the lattice parameter of the seed ribbon, $a_{\parallel}(x) = a_{\text{2D-Si}} * (1-x) + a_{\text{2D-Ge}} * x$, where $a_{\text{2D-Si}}$ and $a_{\text{2D-Ge}}$ denote the lattice parameter of silicene and germanene, respectively.

crossing point of bands forming the upper and the lower Dirac cones.

The effect of strain on the band structure is similar for zigzag and armchair interedges (2D interfaces): in silicene, the tensile strain lowers the local conduction-band minimum at the Brillouin zone center (Γ point). On the contrary, in germanene, the compressive strain raises the local valence-band maximum at the Brillouin zone center.

The electronic band structure of germanene presents a local maximum in the valence band at the Brillouin zone center (Γ point), which, for the free-standing structure, is only 0.45 eV lower than the Fermi energy. As an effect of compressive strain, the local valence-band maximum at Γ increases its energy, and it approaches the value of the Fermi energy at $x \sim 0$. According to our simulations, for $x = 0$ the local valence-band maximum of germanene at the Γ point is -0.02 eV lower than the Fermi energy for the zigzag pseudomorphic growth, and -0.07 eV lower than the Fermi energy for the armchair pseudomorphic growth. In the range considered, therefore, the system does not present a semimetal-to-metal transition that would degrade the carriers population in the Dirac cone; this transition occurs when a local conduction-band minimum or a local valence-band maximum of unstrained band structure becomes degenerate with the Fermi level, due to the effect of the strain on the electronic bands. Our results are in agreement with the *ab initio* data obtained by the local-density approximation for silicene under tensile uniaxial strain in Ref. [26].

To study the strain-induced modification of internal parameters, we consider the variation of the bond length (l_1,l_2) and of the angles formed by different bonds (θ_1, θ_2), as depicted in Fig. 8, where the computed values of θ_1, θ_2, l_1, and l_2 of silicene (central panel) and germanene (right panel) at different x are reported. In the considered range of strain, all internal parameters present a linear variation. For the free-standing structures, the bond length is $l_1 = l_2 = 2.28$ Å for silicene and $l_1 = l_2 = 2.42$ Å for germanene.

For both the zigzag and the armchair interedges (2D interface), the slopes of the functions θ_1, θ_2, l_1, and l_2 of silicene are similar to the corresponding quantities of germanene (the numerical values extracted from the linear fit are displayed in Table I for comparison). The bond angles θ_1,θ_2 as a function of x have complementary behaviors: if one increases, the other decreases by a similar amount to maintain their average $\langle\theta\rangle \equiv (\theta_1 + \theta_2)/2$ almost constant to the free-standing values: $\theta_1 = \theta_2 = 116°14'$ for silicene, $\theta_1 = \theta_2 = 112°19'$ for germanene [with a variation of $\frac{\Delta\langle\theta\rangle}{\langle\theta\rangle} \lesssim 1.6\%$ for zigzag interedge (2D interface), and of $\frac{\Delta\langle\theta\rangle}{\langle\theta\rangle} \lesssim 0.2\%$ for armchair interedge (2D-interface), in the range $0 \leqslant x \leqslant 1$].

The bond angles of both silicene and germanene free-standing crystals have intermediate values between 120°, corresponding to sp^2 bonds of the planar honeycomb structure of graphene, and 109°28′, corresponding to the sp^3 bonds of the diamond structure of bulk silicon and germanium (where each atom is at the center of a tetrahedron formed by its nearest neighbors); this confirms the specific nature of silicene and germanene bonds, having intermediate nature between the sp^2 and sp^3 hybridization.

TABLE I. Linear variation of buckling parameters of silicene and of germanene as a function of the lattice parameter of the seed ribbon, $a_{\parallel}(x) = a_{\text{2D-Si}} * (1-x) + a_{\text{2D-Ge}} * x$, where $a_{\text{2D-Si}}$ and $a_{\text{2D-Ge}}$ denote the lattice parameter of silicene and germanene, respectively.

	Buckling Derivatives			
	zigzag		armch.	
	Si	Ge	Si	Ge
$\partial\theta_1/\partial x$ (deg)	5.30	4.86	−3.25	−3.60
$\partial\theta_2/\partial x$ (deg)	−1.23	−1.31	2.99	2.77
$\partial l_1/\partial x$ (pm)	4.37	4.01	1.31	1.04
$\partial l_2/\partial x$ (pm)	−0.54	−0.03	6.26	5.40

IV. CRITICAL WIDTH

In silicene or germanene epi-ribbons, pseudomorphically grown on a seed ribbon (2D substrate) having a different lattice parameter, the strain energy (i.e., the increase of total energy produced by the strain) increases linearly with the epi-ribbon width. If the epi-ribbon reaches a critical width, w_c, it is energetically convenient for the heterostructure to break the bonds at the interedge (2D interface), thus forming two separate edges (a process that increases the energy) and to release the strain energy (a process that lowers the energy).

We evaluated w_c transposing in two dimensions the method adopted in Refs. [32,33] to compute *ab initio* the critical thickness of 3D epi-layers. An epitaxial ribbon of width w^{epi} can grow pseudomorphically on a seed ribbon (2D substrate) having a different lattice parameter if the following inequality is fulfilled:

$$E^{\text{seed}}_{\text{edge}} + E^{\text{epi}}_{\text{edge}} \geqslant E_{\text{inter}} + \Delta E_{\text{strain}} * w^{\text{epi}}/a_{\perp}. \qquad (2)$$

The equal sign holds if $w^{\text{epi}} = w_c$. The left-hand side of Eq. (2) represents the increase of energy needed to form two noninteracting edges, like the ones displayed in Figs. 3 and 4, and it is given by the sum of the edge energy of the seed ribbon (2D substrate), $E^{\text{seed}}_{\text{edge}}$, plus the edge energy of the epi-ribbon, $E^{\text{epi}}_{\text{edge}}$. The edge energy E_{edge} is the 1D analog of the surface energy in 3D solids [34]. The right-hand side of Eq. (2) represents the sum of the formation energy of the interedge (2D interface), E_{inter}, plus the strain energy of the epi-ribbon of width w^{epi}, pseudomorphically grown from a lattice-mismatched seed ribbon (2D substrate). In Eq. (2), ΔE_{strain} is defined as the difference between the energy (per unit cell) of a strained bulk epi-ribbon [i.e., the unit cell with $a_{\parallel}(x)$ fixed to the corresponding value of the seed ribbon (2D substrate), while the lattice parameter perpendicular to the interedge (2D interface), $a_{\perp}$, is free to relax], minus the energy of the free-standing structure.

V. DISCUSSION

In Fig. 9 we display the results of our simulation for the critical width of a germanene (silicene) epi-ribbon, pseudomorphically grown on a silicene (germanene) seed ribbon (2D substrate), as a function of the lattice parameter of the seed ribbon $a_{\parallel}(x)$. Both zigzag and armchair interedges (2D interface) are considered. According to the convention adopted in the present work, in the horizontal axis, instead of indicating $a_{\parallel}$ as an independent variable, we use for simplicity the parameter x, related to $a_{\parallel}$ through Eq. (1).

The seed ribbon (2D substrate)—except when it is made by silicene at $x = 0$ or by germanene at $x = 1$—is strained because it has an $a_{\parallel}$ that does not correspond to its bulk value; as a consequence, also the seed ribbon has a critical width, w^{seed}_c. If we tune $a_{\parallel}(x)$ by a mechanical stress or by a stripped silicene/germanene geometry, the critical width of the seed ribbon (2D substrate) is equal to the w_c of an epi-ribbon having the same composition, interedge (2D interface), and x of the seed ribbon (2D substrate): $w^{\text{seed}}_c = w^{\text{epi}}_c$. We can assume that this equation is also valid for the case in which we tune $a_{\parallel}(x)$ by lateral growth from a 2D-$Si_{1-x}Ge_x$ sheet [35].

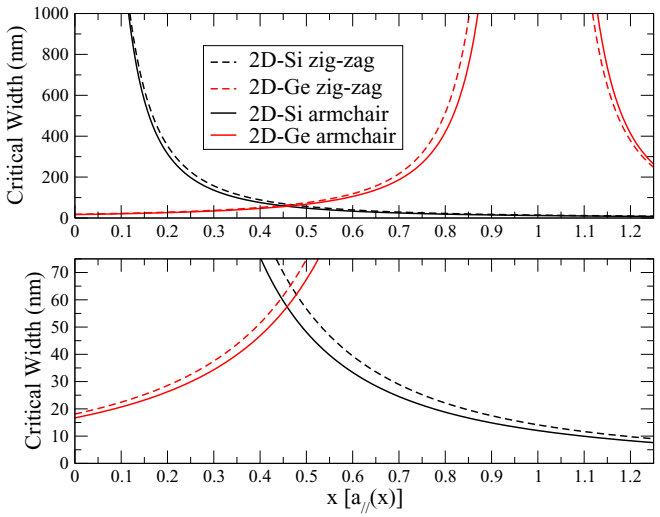

FIG. 9. Critical width as a function of the seed-ribbon lattice parameter $a_{\parallel}$ of silicene (black line) and germanene (red line) for zigzag (dashed line) and for armchair (solid line) interedge (2D interface). Horizontal axis labels correspond to the concentration x according to the relation $a_{\parallel}(x) = a_{\text{2D-Si}} * (1 - x) + a_{\text{2D-Ge}} * x$, where $a_{\text{2D-Si}}$ and $a_{\text{2D-Ge}}$ denote the lattice parameter of silicene and germanene, respectively. In the bottom panel, the vertical scale is magnified.

In Fig. 9 we notice that, in general, for a given x, the critical width of zigzag epi-ribbons is slightly larger than the critical width of armchair epi-ribbons. In particular, for $x = 0$ a ribbon of germanene can pseudomorphically grow on a zigzag (armchair) silicene seed ribbon (2D substrate) up to a critical width of 18 nm (17 nm), while for $x = 1$ a silicene epi-ribbon can pseudomorphically grow on a zigzag (armchair) germanene seed ribbon (2D substrate) up to a critical width of 14 nm (12 nm). These values of the critical width are significantly larger than the experimental data of the critical thickness in conventional 3D Si/Ge heterostructures. For example, in three dimensions the critical thickness of epitaxial growth for germanium on silicon has been reported to be 6 ML = 0.85 nm [36].

If $a_{\parallel}(x)$ is taken halfway between the lattice parameters of free-standing silicene and germanene, the w_c can reach several tens of nanometers: for $x \simeq 0.5$ both silicene and germanene ribbons have a critical width of about 50–70 nm, i.e., about one order of magnitude larger than the present resolution of the lithographic techniques.

To quantify the state-of-the-art lithographic resolution, we consider the extreme ultraviolet lithography, a technique exploitable in industrial processes. Recently, by extreme ultraviolet lithography, Mojard *et al.* obtained patterning with 7 nm resolution, while the intrinsic resolution limit of this lithographic technique (at 13.5 nm wavelength) is ∼3.5 nm [37]. Other lithographic techniques employing shorter wavelengths, such as ion-beam lithography or electron-beam lithography, can reach a resolution of a few nanometers.

Thus, it is possible to envisage lithographically patterned silicene/germanene lateral heterostructures, where the electronic band structure can be engineered by the "geometrical

shape" of the heterostructure, by combining silicene and germanene ribbons of different width.

In the present work, we investigated the simplest geometry, which is based on striped 2D-PHs, made by alternating silicene and germanene ribbons. In this 2D-PHs, the width of each ribbon (made of silicene or of germanene) is constant along the entire ribbon length; however, the width of silicene ribbons may be different from the width of germanene ribbons (as in 3D Si/Ge superlattices [12]). With this geometrical arrangement, the desired $a_{\parallel}$ is determined by the ratio of silicene and germanene width. If a tensile stress is applied to the two ends of the ribbons in the striped 2D-PHs, it is possible to tune "on demand" the $a_{\parallel}$ and, therefore, to vary continuously the electronic band structures.

While in 3D growth the techniques (MBE,CVD) commonly used to build superlattices produce epi-layers unstrained along the growth direction, in 2D growth the use of lithographic techniques allows us—in principle—to pattern planar heterostructure composed of pseudomorphic flakes having a more general shape, which can be strained in the 2D plane along two different directions (e.g., along $a_{\parallel}$ and along $a_{\perp}$). This possibility paves the way for the intriguing opportunity to create 2D-PHs containing quantum dots or quantum wells whose electronic properties may depend on the planar shape of the dot or of the well. Although the experimental realization of these foreseen 2D-PHs can be a formidable task for the present or near-future technology, a lateral heterostructure based on $MoSe_2$-WSe_2 has been already synthesized [38].

As mentioned in Sec. III, a compressive strain can eventually produce a corrugation in germanene sheets, so, in the following, we will give a brief discussion about how the rippling of germanene can affect our results, and we provide a hint as to how we may overcome this problem. We have two cases. Case I: the regime where germanene rippling is absent or negligible. For x close to $x \sim 1$ or $x \geqslant 1$, no compressive strain is present and the 2D-PHs should be planar with critical width described according to our model. Also in the case of germanene ribbons having small width (i.e., embedded in a silicene layer of macroscopic size), due to the pseudomorphic constraint at the interedge with silicene, the rippling of germanene is expected to be unlikely. Case II: the regime where germanene rippling is possible. For $x \ll 1$ and for germanene ribbons having large width, there is the possibility that in the region far from the interedges, the germanene ripples. However, the rippling of the germanene ribbon releases the constraint imposed in Eq. (2), thus lowering the strain energy of the germanene epi-ribbon. As a consequence, the critical width of a rippled germanene epi-ribbon is expected be larger than the one we estimated for a planar germanene epi-ribbon; so the germanene w_c reported in Fig. 9 in the range $0 \leqslant x < 1$ can be considered as a lower bond for the critical width of rippled germanene. We note that, according to Fig. 8, the structural parameters are linear as a function of x; as a consequence, the structural parameters of a rippled germanene are expected to assume intermediate values between the value predicted for planar compressed germanene and the free-standing one.

Further, we suggest that the use of a capping monolayer can prevent the oxidation of silicene/germanene 2D-PHs; in addition, a capping monolayer can also prevent the formation of germanene ripples: in Ref. [39], *ab initio* simulations show that a bilayer formed by germanene/graphene is structurally stable for a germanene lattice parameter compressed by about -2%. In silicene/germanene 2D-PHs, a compression of -2% in the lattice parameter $a_{\parallel}(x)$ of germanene corresponds to $x \sim 0.5$. At this value of x, both silicene and germanene ribbons have a critical width of several tens of nanometers.

VI. CONCLUSION

In conclusion, the present study proposes a type of 2D heterostructure that is formed by alternating stripes of silicene and germanene ribbons. We computed *ab initio* the effect of strain on the structural and electronic properties of these ribbons, and we predicted that in these 2D-PHs the ribbons of silicene and germanene remain lattice-matched at the interedge (2D interface) also for a ribbon width well above the present resolution of lithographic techniques. Thus, it is possible to envisage lithographically patterned silicene/germanene lateral heterostructures where the electronic band structure can be engineered through the geometrical shape of 2D-PHs, through mechanical stress, or through both. We expect that critical widths similar to those found in the present work can also be obtained for semiconducting silicane and germanane, the H-passivated silicene and germanene, which can be used as an alternative to (or in combination with) silicene or germanene to build semiconductor/semiconductor (or semiconductor/semimetal) 2D-PHs.

Future progress in this area of research in nanoelectronics may lead to the development of 2D junctions in which the Fermi velocity of high-mobility carriers in the Dirac cone can be tuned "on demand," e.g., by a mechanical strain, in 2D-PHs. Our results may pave the way for novel planar heterostructures that can be used as building blocks in ultimate-scaled devices in future 2D electronics.

ACKNOWLEDGMENTS

We acknowledge the CINECA and the Regione Lombardia award under the LISA initiative for providing high-performance computing resources and support, G. Onida for helpful discussions, M. Longo for a critical reading of the manuscript, and R. Colnaghi for technical support on the computer hardware.

[1] F. Bonaccorso, L. Colombo, G. Yu, M. Stoller, V. Tozzini, A. C. Ferrari, R. S. Ruoff, and V. Pellegrini, Science **347**, 41 (2015).

[2] C.-C. Liu, W. Feng, and Y. Yao, Phys. Rev. Lett. **107**, 076802 (2011).

[3] A. Dimoulas, Microelectron. Eng. **131**, 68 (2015).

[4] A. Kara, H. Enriquez, A. P. Seitsonen, L. C. Lew, Yan Voom, S. Vizzini, B. Aufray, and H. Oughaddou, Surf. Sci. Rep. **67**, 1 (2012).

[5] M. Houssa, A. Dimoulas, and A. Molle, J. Phys.: Condens. Matter **27**, 253002 (2015).

[6] M. Derivaz, D. Dentel, R. Stephan, M.-C. Hanf, A. Mehdaoui, P. Sonnet, and C. Pirri, Nano Lett. **15**, 2510 (2015).

[7] L. Tau, E. Cinquanta, D. Chiappe, C. Grazianetti, M. Fanciulli, M. Dubey, A. Molle, and D. Akinwande, Nat. Nanotechnol. **10**, 227 (2015).

[8] S. Cahangirov, M. Topsakal, E. Aktürk, H. Sahin, and S. Ciraci, Phys. Rev. Lett. **102**, 236804 (2009).

[9] M. Topsakal and S. Ciraci, Phys. Rev. B **81**, 024107 (2010).

[10] N. Jung, N. Kim, S. Jockusch, J. N. Turro, P. Kim, and L. Brus, Nano Lett. **9**, 4133 (2009).

[11] A. K. Geim and K. S. Novoselov, Nat. Mater. **6**, 183 (2007).

[12] P. Y. Yu and M. Cardona, *Fundamentals of Semiconductors* (Springer, Heidelberg, 2010).

[13] From the Latin words *ex*[from]-*margo, marginis*[edge].

[14] Due to the flexibility of the lithographic technique, the above growth process can be generalized to produce a ribbon of arbitrary shape

[15] P. Giannozzi, S. Baroni, N. Bonini, M. Calandra, R. Car, C. Cavazzoni, D. Ceresoli, G. L. Chiarotti, M. Cococcioni, I. Dabo, A. Dal Corso, S. Fabris, G. Fratesi, S. de Gironcoli, R. Gebauer, U. Gerstmann, C. Gougoussis, A. Kokalj, M. Lazzeri, L. Martin-Samos, N. Marzari, F. Mauri, R. Mazzarello, S. Paolini, A. Pasquarello, L. Paulatto, C. Sbraccia, S. Scandolo, G. Sclauzero, A. P. Seitsonen, A. Smogunov, P. Umari, and R. M. Wentzcovitch, J. Phys.: Condens. Matter **21**, 395502 (2009).

[16] J. P. Perdew, K. Burke, and M. Ernzerhof, Phys. Rev. Lett. **77**, 3865 (1996).

[17] P. Hohenberg and W. Kohn, Phys. Rev. **136**, B864 (1964).

[18] W. Kohn and L. J. Sham, Phys. Rev. **140**, A1133 (1965).

[19] A. M. Rappe, K. M. Rabe, E. Kaxiras, and J. D. Joannopoulos, Phys. Rev. B **41**, 1227 (1990).

[20] D. Vanderbilt, Phys. Rev. B **41**, 7892(R) (1990).

[21] H. J. Monkhorst and J. D. Pack, Phys. Rev. B **13**, 5188 (1976).

[22] L. Marchetti, Master's thesis, Università Statale degli Studi di Milano, 2014.

[23] J-A. Yan, S-P. Gao, R. Stein, and G. Coard, Phys. Rev. B **91**, 245403 (2015).

[24] Q.-X. Pei, T.-W. Zhang, Z-D. Sha, and V. B. Shenoy, J. Appl. Phys. **114**, 033526 (2013).

[25] M. Hu, X. Zhang, and D. Poulikakos, Phys. Rev. B **87**, 195417 (2013).

[26] R. Qin, W. Zhu, Y. Zhang, and X. Deng, Nanoscale Res. Lett. **9**, 521 (2014).

[27] R. Qin, C.-H. Wang, W. Zhu, and Y. Zhang, AIP Adv. **2**, 022159 (2012).

[28] T. P. Kaloni, Y. C. Cheng, and U. Schwingensclögl, J. Appl. Phys. **113**, 104305 (2013)

[29] G. Liu, M. S. Wu, C. Y. Ouyang, and B. Xu, Europhys. Lett. **99**, 17010 (2012).

[30] Y. Wang and Y. Ding, Solid State Commun. **155**, 6 (2013).

[31] Preliminary calculations with supercell techniques confirm this assumption; A. Debernardi (unpublished).

[32] V. Fiorentini and G. Gulleri, Phys. Rev. Lett. **89**, 266101 (2002).

[33] A. Debernardi, C. Wiemer, and M. Fanciulli, Phys. Rev. B **76**, 155405 (2007).

[34] A. Pimpinelli and J. Villain, *Physics of Crystal Growth* (Cambridge University Press, Cambridge, 1998).

[35] Truly, if $a_{\parallel}(x)$ is tuned by lateral growth from a 2D-$Si_{1-x}Ge_x$ sheet, we should expect that w_c^{seed} may be even larger than w_c^{epi}, because for a given interedge (2D-interface) (zigzag, armchair) and for fixed $a_{\parallel}(x)$, the interedge (2D-interface) energy of a sharp Si/Ge junction is expected to be larger than the interedge (2D-interface) energy of $Si/Si_{1-x}Ge_x$ and of $Ge/Si_{1-x}Ge_x$ junction, while E_{edge} of the 2D-$Si_{1-x}Ge_x$ sheet is expected to be of the same order of magnitude as the ones of silicene and germanene. With these assumptions, the inequality $w_c^{\text{seed}} \gtrsim w_c^{\text{epi}}$ follows from Eq. (2).

[36] K. Sasaki, Y. Takahashi, T. Ikeda, and T. Hata, Vacuum **66**, 457 (2002).

[37] N. Mojarad, M. Hojeij, L. Wang, J. Gobrecht, and Y. Ekinci, Nanoscale **7**, 4031 (2015).

[38] C. Huang, S. Wu, A. N. Sanchez, J. P. Peters, R. Beanland, J. S. Ross, P. Rivera, W. Yao, D. H. Cobden, and X. Xu, Nat. Mater. **13**, 1096 (2014).

[39] Y. Cai, C.-P. Chuu, C. M. Wei, and M. Y. Chou, Phys. Rev. B **88**, 245408 (2013).